

## Integrated research on power generation and heat extraction with an increasing-pressure endothermic process in a downhole heat exchanger

Hao Yu<sup>1</sup>, Xinli Lu<sup>1\*</sup>, Jiali Liu<sup>1</sup>, Chenchen Li<sup>1</sup>, and Shuhui Li<sup>1</sup>

<sup>1</sup> Key Laboratory of Efficient Utilization of Low and Medium Grade Energy, MOE  
Tianjin University, 135 YaGuan Road, Jinnan District, Tianjin 300350, China

\*Corresponding author email address: xinli.lu@tju.edu.cn,

**Keywords:** Geothermal Power Generation, Heat Extraction System, Downhole Heat Exchanger

### ABSTRACT

There are plenty hot dry rock (HDR) resources in the range of 3-10 km underground. Seeking economical and efficient utilization scheme of using hot dry rock resources is an effective way to solve the shortage of energy supply. In this study, a novel power cycle, with an increasing-pressure endothermic process in the downhole heat exchanger (DHE) and CO<sub>2</sub>-based mixture as working fluid, has been developed for the geo-fluid temperature ranging from 100 °C to 200 °C. The adopted CO<sub>2</sub>-based mixture has a higher critical temperature and hence can be condensed under ambient temperature condition. It has been found that the endothermic process in the DHE and exothermic process in the condenser have a better match with the temperature change of the heat source (geo-fluid) and that of the cooling water respectively, which reduces the heat transfer irreversibility. The maximum net power output has been chosen as an objective function in this study. The operation parameters of the power generation system and the structural size of the DHE have been optimized simultaneously. The thermodynamic performance of the proposed novel power cycle has been compared with flash-steam system and Organic Rankine Cycle (ORC) under same operation conditions.

### 1. INTRODUCTION

Geothermal energy plays a very important role in the energy basket of the world. For example, it has been estimated that the total heat available in the crust of the earth, is around  $540 \times 10^7$  EJ (Olasolo et al., 2016). Enhanced geothermal system (EGS) will play an important role in the future of renewable energy. EGS systems are buried at a depth more than 3 km which bears temperature more than 150 °C (Zheng et al., 2021). Indirect and direct applications like power generation, food drying, aquaculture, vegetable cultivation, heating and cooling etc. are possible by extracting the hot water/steam (Sircar et al., 2022). The key to success is to expand the fracture network. Hydraulic fracturing is a widely used technology in hydrocarbon field where permeability is low.

The downhole coaxial heat exchanger (DCHE) geothermal system, which injects and heats working fluids through the annulus and produces them through the insulated inner pipe, is suitable for developing medium deep geothermal resources (Zhang et al., 2019). Alternatively, a single-well closed-loop geothermal system, wherein the direct contact between the fluid and the geothermal reservoir is avoided, provides a better solution. Because only heat is brought to the surface without any underground minerals, its impact on the environment is negligible. Many studies have been conducted on the heat extraction performance of DCHEs, owing to their relatively large heat exchange areas, high thermal power, and lower construction costs. Holmberg et al. (2016) found that the thermal power of a DCHE system is higher than that of the conventional U-tube well (borehole heat exchanger system). Acuna (2010) compared the performance of a U-type and a coaxial DHE. The results indicated that the coaxial DHE decreased pressure drop by 65% at a variety of flowrates compared with U-type.

In terms of geothermal power generation, Organic Rankine Cycle (ORC) is widely used for medium or low temperature geo-fluid (Khosravi et al., 2019). Trans-critical Rankine Cycle (TRC) has an advantage in reducing the heat transfer irreversibility when the supercritical working fluid is gaining heat from the heat source, because the temperature of the working fluid is not constant during this heating process, which has a better match with the heat source temperature change (Karellas et al., 2008). Landelle et al. (2017) carried out an experimental investigation of a TORC, they found that TORC shows a good potential for waste heat recovery application since it performed better than  $\frac{2}{3}$  of the same power scale ORC for gross exergetic recovery efficiency.

CO<sub>2</sub> has good mobility and excellent heat transfer performance, so it has been considered to be a suitable working fluid for geothermal power generation. Due to the low critical temperature of CO<sub>2</sub> (Condensation is difficult at room temperature), it is usually considered to add another working fluid with higher critical temperature to CO<sub>2</sub>. Wu et al. (2017) found that when the geo-fluid temperature is between 100-150 °C, R161/CO<sub>2</sub> is the best working fluid for trans-critical power cycle (TPC) in terms of both thermodynamic economic performances. Pan et al. (2015) pointed out that using R290/CO<sub>2</sub> mixture fluid can solve the problem that subcritical CO<sub>2</sub> is hardly condensed by conventional cooling water. The maximum thermal efficiency and the maximum net power output of the trans-critical power cycle increase with the increase of mass fraction of R290.

The aim of this study is to develop a power cycle (with an increasing-pressure endothermic process) for enhanced geothermal systems, with particular reference to the medium or low geofluid temperature. Differ from the working fluid (pure CO<sub>2</sub>) and the power cycle (Brayton cycle) that Amaya et al. (2020) adopted, in this study, CO<sub>2</sub>-based mixture working fluids were investigated and a different power cycle was configured.

## 2. SYSTEM DESCRIPTION

### 2.1 Physical model

The schematic of the Increasing-Pressure Endothermic Cycle (IPC) is shown in Fig.1a, and the temperature-entropy (T-s) diagram of the power generation system is shown in Fig.1b. The Increasing-Pressure Endothermic Cycle (IPC) consists of underground downhole heat exchanger (DHE) and above-ground power generation system.

The liquid CO<sub>2</sub>-based mixture from the condenser is pressurized into supercritical state (process 1-2) and is then injected into the DHE annular region of outer tube. The downward annulus flow absorbs heat from the upward flowing geo-water outside the DHE, as the Fig.1b process 2-3 shown. The inner and outer pipes of the DHE are connected in the bottom area, the working fluid that extracted heat passes upward from the bottom to the top (process 3-4) in the inner pipe. The working fluid from DHE enters the turbine to drive the generator for electricity generation (process 4-5). The turbine exhaust (state 5) flows into the condenser where it is condensed into complete saturated liquid (state 1), then another cycle.

The downward working fluid (CO<sub>2</sub>-based mixture) and the upward geo-water form a counter-flow in the production well, which makes the heat exchange more adequate. As the appellation of the cycle (Increasing-Pressure Endothermic Cycle) reveals that the most important feature of this cycle lies in its increasing-pressure endothermic process (process 2-3), which is determined based on the heat transfer model shown in next section. Only in the large-scale closed-loop DHE, the gravitational potential energy works on the working fluid so it can absorb heat and increase pressure at the same time. The red line in Fig.1b is the Increasing-Pressure Endothermic process, which is differ from the heat absorption of working fluid in traditional ORC system. Due to the difference in working fluid density between the upward and downward tubes, the buoyancy-driven thermosiphon effect in the DHE can boost the working-fluid's DHE outlet pressure. Hence, the IPC power generation performance can be improved.

Due to the existence of temperature glide, the zeotropic working fluid can better match the cold source in the condensation process. CO<sub>2</sub>-based mixtures are selected as working fluids in this study. Thermal properties, toxicity, flammability and environmental friendliness have been considered in the selection of Organic working fluid. Seven Organic working fluids (R161, R32, R134a, R152a, R600a, R1234yf, and R601a) were selected in this article, the thermal-physical parameters are shown in table 1.

**Table 1 Thermal-physical parameters of the organic working fluids.**

Substance	Critical temperature ( $t_c$ , °C)	Critical pressure ( $p_c$ , MPa)	ODP	GWP	Atmospheric life (years)	Security
R161	102.2	5.09	0	12	0.21	-
R32	78.1	5.78	0	675	4.9	A2
R134a	101.1	4.06	0	1370	14.0	A1
R152a	113.3	4.52	0	124	1.4	A2
R600a	135.0	3.53	0	3	-	A3
R1234yf	94.7	3.38	0	4.4	0.029	A2L
R601a	187.2	3.47	0	-	-	A3

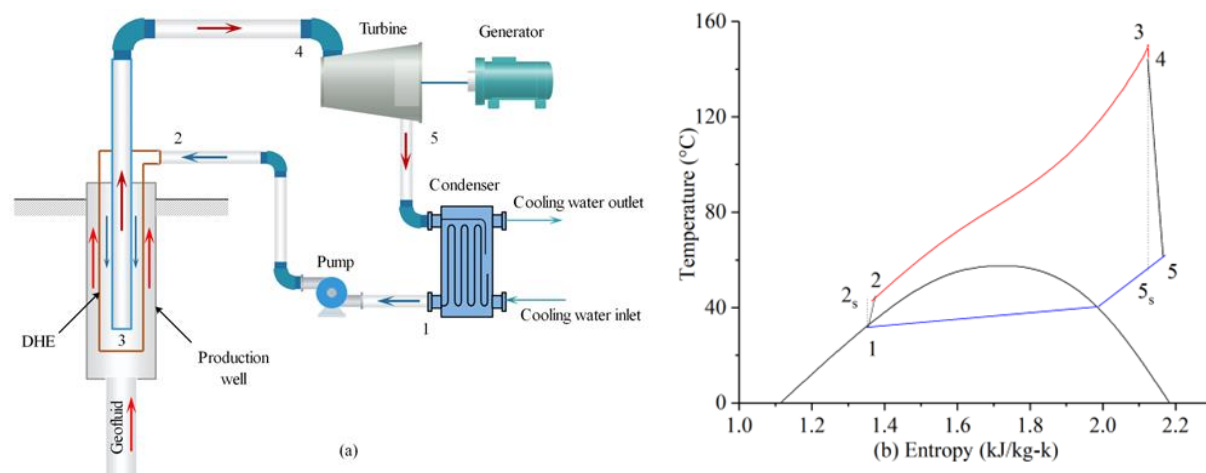


**Figure 1 Schematic and Temperature-entropy diagrams of the Increasing-pressure endothermic power generation system.**

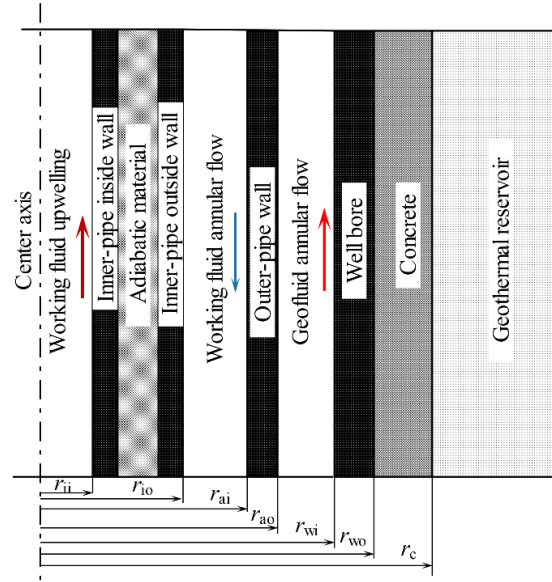


**Figure 2 Schematic diagram of the DHE and production well.**

Fig.2 shows the schematic diagram of DHE and production well, the thermal insulation layer between the inner-pipe inside wall and the inner-pipe outside wall is filled with adiabatic material. Table 2 shows the parameters used in the simulation.

**Table 2 parameters used in the simulation**

Items	Parameters
Turbine isentropic efficiency, $\eta_t$	0.85
Pump isentropic efficiency, $\eta_p$	0.8
Outlet temperature of condenser, $t_{co}$ (°C)	25
Inner-pipe inside wall diameter, $d_{ii}$ (m)	0.073
Inner-pipe outside wall diameter, $d_{io}$ (m)	0.089
Annulus-pipe inside wall diameter, $d_{ai}$ (m)	0.12
Annulus-pipe outside wall diameter, $d_{ao}$ (m)	0.138
Wellbore inside diameter, $d_{wi}$ (m)	0.215
Wellbore outside diameter, $d_{wo}$ (m)	0.235
Density of rock, $\rho_e$ (kg/m <sup>3</sup> )	2650
Heat capacity of rock, $c_e$ (J/kg·k)	837
Thermal conductivity of rock, $\lambda_e$ (W/m·k)	2.5
Thermal conductivity of casing, $\lambda_{ca}$ (W/m·k)	30
Thermal conductivity of insulated tube, $\lambda_t$ (W/m·k)	0.02
Thermal conductivity of cement, $\lambda_{ce}$ (W/m·k)	0.72

## 2.2 Thermodynamic model

As the coaxial DHE and the production well are concentric, the 3-D heat transfer model has been simplified to a radially symmetric model. The heat transfer covers the following aspects: heat transfer between the inner pipe and the outer pipe of the DHE, heat transfer between the DHE and the geo-fluid, heat transfer between the geo-fluid and rock, and the heat transfer in the rock.

### 2.2.1 Power generation system

Thermodynamic modeling of the IPC has been carried out based on the following assumptions:

- (1) All components of the system are operating in under steady state;
- (2) In the above-ground equipment, heat losses and mixture fraction losses in pipes are ignored;

- (3) The injection pressure of CO<sub>2</sub>-based mixture is higher than its critical pressure;
- (4) The CO<sub>2</sub>-based mixture is in a saturated liquid state at the pump inlet.

In this study, all the thermodynamic and transport properties of the mixtures have been calculated by calling the database of National Institute of Standards and Technology (NIST) using REFPROP 10. The accuracy of each calculated property basically depends on the binary interaction parameter that is fitted by experimental data.

The turbine-generator power output can be calculated as follow:

$$W_g = m \times (h_4 - h_5) \times \eta_t \quad (1)$$

The condensation process of the CO<sub>2</sub>-based mixture is non-isothermal showing the existence of a temperature glide, which makes a better match between the working fluid temperature drop with the temperature rising of the cooling water and results in a less heat transfer irreversibility. The heat balance in the condenser is shown below:

$$Q_C = m \times (h_5 - h_1) \quad (2)$$

$$m_C = m \times (h_1 - h_5) / (h_{C,out} - h_{C,in}) \quad (3)$$

The power consumption of injection pump is given by:

$$W_p = m \times (h_2 - h_1) \quad (4)$$

The net power output of the system is equal to the power generated minus the pump work, is given by:

$$W_{net} = W_g - W_p \quad (5)$$

### 2.2.2 DHE model

The overall heat transfer model has been coupled with the flow model and calculated by the finite difference method. The temperature and pressure distributions of the working fluid as well as the geo-fluid are coupled and solved at the same time. The mass equation and the momentum equation can be simplified as:

$$\frac{d}{dz}(\rho v) = 0 \quad (6)$$

$$\frac{dp}{dz} = \pm \rho g \sin \theta - \rho v \frac{dv}{dz} - f \frac{\rho v^2}{2d} \quad (7)$$

The energy conservation equation of the working fluids can be written as follow:

$$\frac{dh}{dz} = \pm g \sin \theta - v \frac{dv}{dz} - \frac{q}{w} \quad (8)$$

$$\frac{dT}{dz} = -\frac{q}{wc_p} + \frac{1}{c_p} \left( \eta c_p \frac{dp}{dz} \pm g \sin \theta - v \frac{dv}{dz} \right) \quad (9)$$

## 3. RESULTS

In this section, the thermodynamic optimization of the IPC has been carried out, including comparison of the working fluids, optimization of the system parameter, and analysis of the effect of the DHE structure size on IPC power generation. Based on the thermodynamic optimization of the power generation system, the net power generation of IPC has been compared with that of ORC, trans-critical CO<sub>2</sub> (t-CO<sub>2</sub>) cycle and single-flash (SF) system.

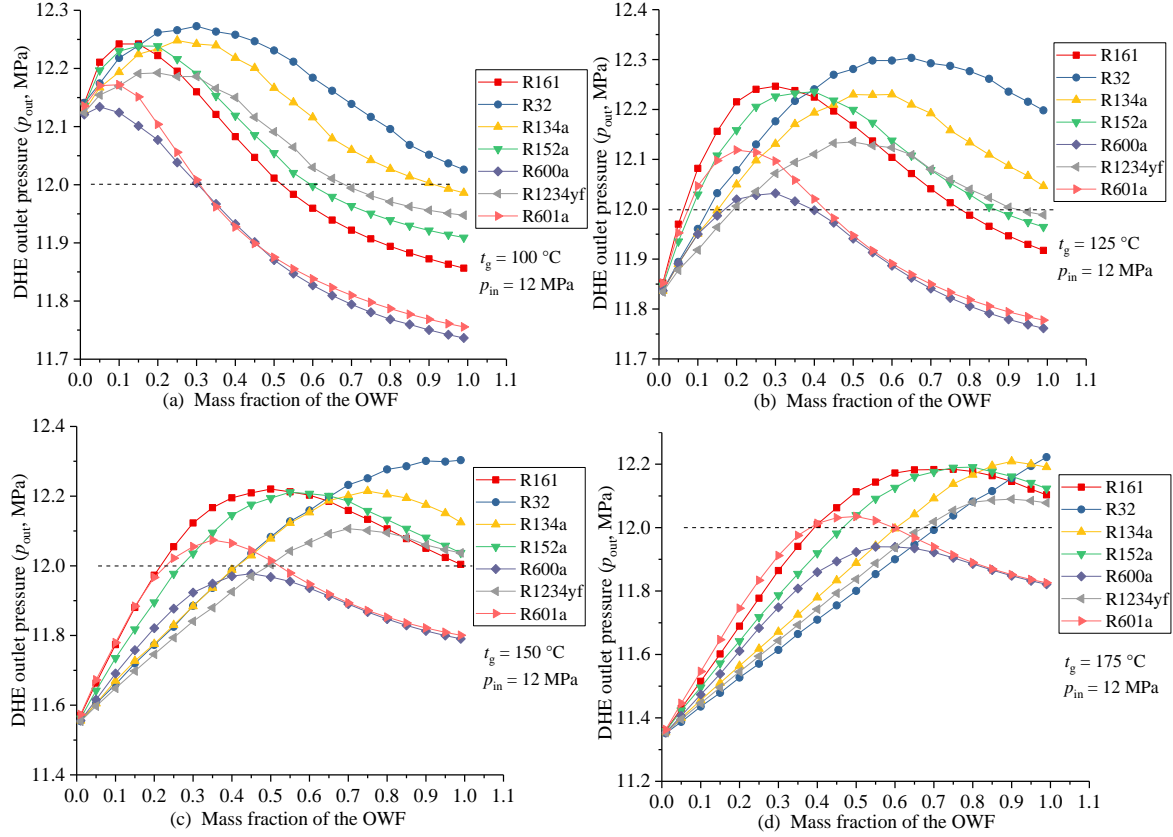
### 3.1 Comparison of IPC using different CO<sub>2</sub>-based working fluids

Figure 3 shows the effect of mass fraction on the DHE working fluid outlet pressure ( $p_{out}$ ). The geo-fluid temperature ( $t_g$ ) equals 100 °C, 125 °C, 150 °C, and 175 °C, respectively, with DHE inlet pressure ( $p_{in}$ ) maintained at 12 MPa.

When the  $t_g$  is 100 °C (Figure 3a), the DHE outlet pressure increase firstly and then decrease with the increase of mass fraction of OWF in all CO<sub>2</sub>-based mixtures. There is an optimal mass fraction of the mixture at a given  $t_g$  to maximize the  $p_{out}$ . At some mass fraction, the  $p_{out}$  is greater than the  $p_{in}$  (black dot line), which means the CO<sub>2</sub>-based mixture can make full use of the thermal siphon effect to reduce the pump power consumption. At all mass fractions, the  $p_{out}$  of DHE using CO<sub>2</sub>-R32 is higher than the  $p_{in}$  and, under most conditions, higher than that of other mixtures. As the temperature increases, take 125 °C as an example (Figure 3b), the optimal mass fraction associated with maximum  $p_{out}$  shifts to the right. The trend is the same when the  $t_g$  increase to 150 °C and 175 °C, except that the higher the  $t_g$ , the smaller the range of mass fraction in which the  $p_{out} > p_{in}$ . it is worth noting that when the  $t_g$  is 175 °C, the higher mass fraction of R32 in mixture, the more pressure increasement (almost linearly), see Figure 3d.

The IPC net power output ( $W_{\text{net}}$ ) with respect to different CO<sub>2</sub>-based mixtures and mass fraction of OWF/CO<sub>2</sub> are shown as Figure 4. When the  $t_g$  is 100 °C and the mass fraction of OWF in all mixtures is 0, the net power generation of the system is the maximum (Figure 4a). Which means that at this temperature, pure CO<sub>2</sub> should be used for better power generation performance than the CO<sub>2</sub>-based mixture. As the temperature increases, the optimal mass fraction associated with maximum  $W_{\text{net}}$  shifts to the right. Taking R32/CO<sub>2</sub> as an example, when the  $W_{\text{net}}$  reach the highest point under the condition of  $t_g = 125$  °C (Figure 4b), the mass fraction of R32/CO<sub>2</sub> is 0.35/0.65; when the  $W_{\text{net}}$  reach the highest point under the condition of  $t_g = 150$  °C (Figure 4c), the mass fraction of R32/CO<sub>2</sub> close to 1/0. It should be noted that when the  $t_g$  is 150 °C, after the mass fraction of R32 increases to 0.6 and then continues to increase, the  $W_{\text{net}}$  increases little.

The  $W_{\text{net}}$  of IPC using R600a/CO<sub>2</sub> and R601a/CO<sub>2</sub> as working fluid are the lowest two in most operation conditions, especially when the mass fraction is around 0.9.



**Figure 3** DHE outlet pressure tendency with respect to different CO<sub>2</sub>-based mixture working fluids and mass fraction of OWF/CO<sub>2</sub>.

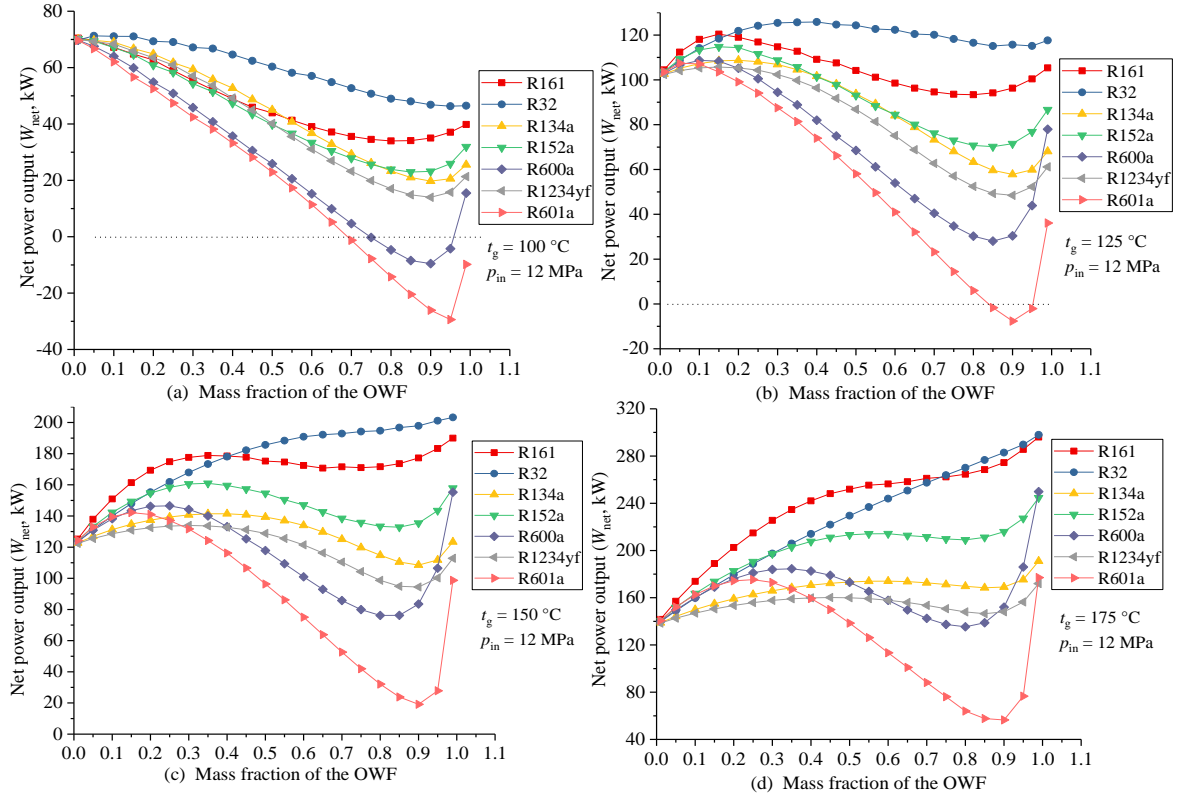


**Figure 4** IPC net power output tendency with respect to different CO<sub>2</sub>-based mixture working fluids and mass fraction of OWF/CO<sub>2</sub>.

### 3.2 Optimization of operation parameter

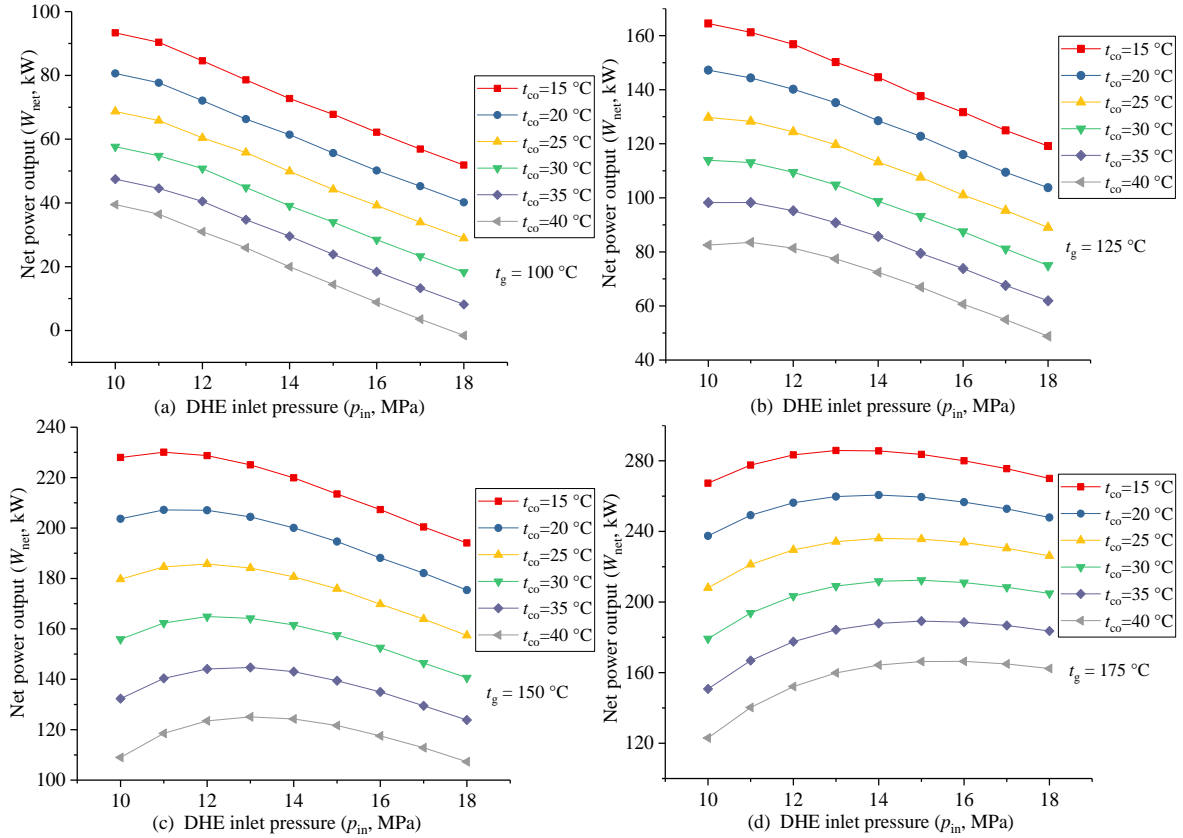
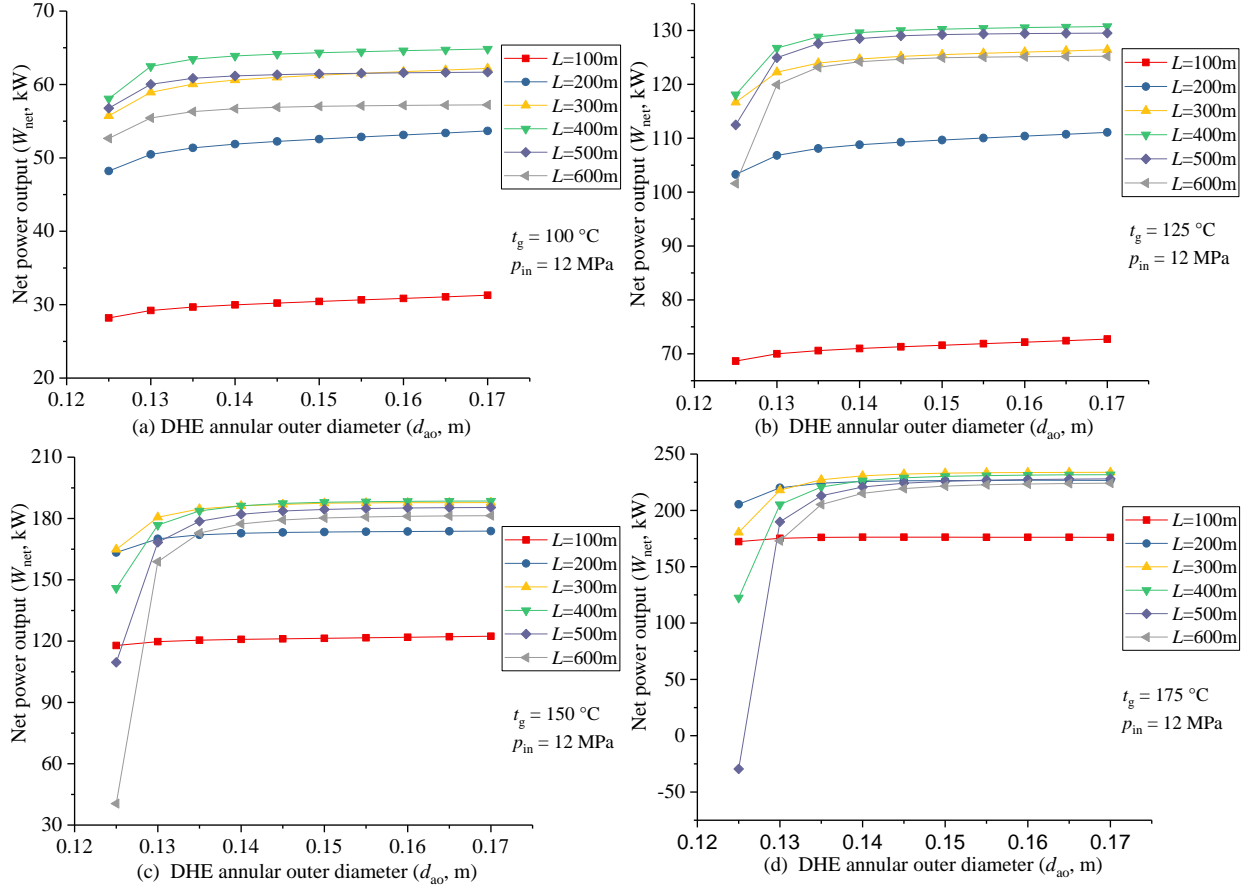


**Figure 5** IPC net power output tendency with respect to different DHE inlet pressure and condensation temperature ( $m_g = 5$  kg/s,  $m_m = 5$  kg/s, mass fraction of R32/CO<sub>2</sub> = 0.5/0.5).

The effect of IPC operation parameter (inlet pressure of DHE and outlet temperature of condenser) on net power output is shown in Figure 5. Reducing the  $t_{co}$  can effectively increase the  $W_{net}$  of the IPC system, which indicates that the lower DHE injection temperature does not necessarily reduce the power output of the system. At low geo-fluid temperature, the  $W_{net}$  decreases with the increase of DHE inlet pressure ( $p_{in}$ ) within the scope of our study, see Figure 5a, b. However, when the temperature increases, there is an optimal DHE inlet pressure that maximizes the  $W_{net}$ , shown as Figure 5c, d. The higher the geo-fluid temperature, the higher the optimal DHE inlet pressure.

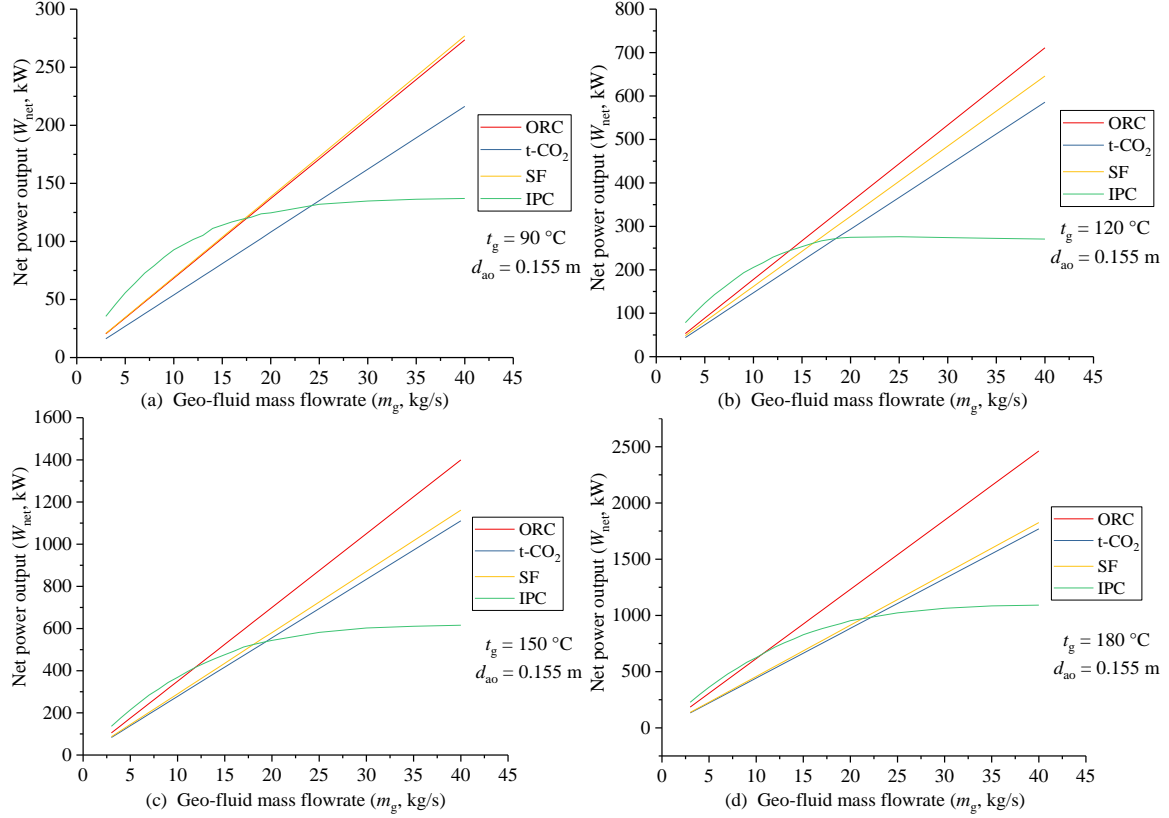
### 3.3 Effect of the DHE structure size

Figure 6 shows the IPC net power output tendency with respect to DHE length ( $L$ ) and annulus-pipe outside wall diameter ( $d_{ao}$ ). Increasing the  $d_{ao}$  and  $L$  will increase the heat exchange area of the DHE, making the heat exchange between the CO<sub>2</sub>-based mixture and geo-fluid more adequate, and to a certain extent will increase the working fluid temperature of the DHE outlet and then enhance the power generation. It can be seen that, when the  $L$  is 100m, the net power output is far less than the other length condition. When the  $d_{ao}$  is constant, the increase of  $L$  will result in an increase of the  $W_{net}$ , and gradually decreases after 400 m.; when the  $L$  is constant, the  $W_{net}$  increases with the increase of the  $d_{ao}$ , and then flattens out (if  $d_{ao} > 0.14$  m).



**Figure 6** IPC net power output tendency with respect to  $L$  and  $d_{ao}$  ( $m_g = 5$  kg/s, mass fraction of R32/CO<sub>2</sub> = 0.5/0.5).

### 3.3 Effect of the DHE structure size



**Figure 7** Net power output comparisons among various geothermal power generation systems with respect to different geo-fluid temperatures ( $t_g$ ) and mass flowrate ( $m_g$ ).

Comparison of the net power output between the ORC, t-CO<sub>2</sub>, SF and IPC systems connects with different geo-fluid temperatures and mass flowrate (Figure 7). All four systems have attained their optimum operation conditions. The net power output of the ORC and SF is almost the same, when the  $t_g$  is 90 °C (Figure 7a); is always higher than that of the t-CO<sub>2</sub>. With the increase of geo-fluid mass flowrate ( $m_g$ ), the power generation of IPC system firstly increased and then remained constant. This is mainly due to the limited DHE are, so that the heat exchange does not increase exponentially with the increase of  $m_g$ . When the  $m_g$  is 17.5 kg/s, the  $W_{net}$  of ORC, SF and IPC are the same; When the  $m_g$  is 24 kg/s, the  $W_{net}$  of t-CO<sub>2</sub> and IPC are equal.

When the  $t_g$  is 120 °C (Figure 7b), the  $W_{net}$  of SF is between that of ORC and t-CO<sub>2</sub>, and the curve of SF deviates from ORC to t-CO<sub>2</sub> with the increase of  $t_g$  (see Figure 7c, d). What is worth noticing is that the higher the geo-fluid temperature, the smaller the geo-fluid mass flowrate range in which IPC systems shows advantage over other systems (the  $W_{net}$  of IPC is the highest).

### 4. CONCLUSION

In this study, an increasing-pressure endothermic cycle (IPC) using geo-fluid in an artesian geothermal well to generate electricity has been investigated. The power generation performance of the IPC has been investigated by analyzing the impacts of the following important parameters: mass fraction and varieties of the CO<sub>2</sub>-based mixtures, condenser working fluid outlet temperature and DHE working fluid inlet pressure, the DHE length and annulus-pipe outside wall diameter. In addition, thermodynamic performance (in terms of the net power output) has been compared among the IPC, conventional organic Rankine cycle (ORC), trans-critical CO<sub>2</sub> (t-CO<sub>2</sub>) system and single-flash (SF) system. The following conclusions can be drawn from this study:

- (1) An increasing-pressure endothermic cycle has been developed using a large scale DHE and CO<sub>2</sub>-based mixture. The non-isothermal condensation process can be achieved by using zeotropic mixture working fluids. The temperature variation between working fluid and cooling water can be better matched, and the area of condenser can be reduced;
- (2) The increasing-pressure endothermic process of working fluid in the DHE has a better match with the temperature change of the geo-fluid, which reduces the heat transfer irreversibility and improves the power generation;
- (3) Comparison of net power output among seven different CO<sub>2</sub>-based mixture with respect to different geo-fluid temperatures shows that using the mixture working fluid of R32/CO<sub>2</sub> has better thermodynamic performance than others;
- (4) Numerical study shows that a longer DHE or a larger DHE diameter associated with a lower DHE inlet temperature can improve the IPC power production performance;
- (5) In terms of power generation, IPC shows advantages under small geo-fluid flowrate conditions compared with other systems.



## ACKNOWLEDGMENTS:

The work was supported by the National Key Research and Development Program of the 13th Five-Year Plan of China (Grant No. 2018YFB1501805).

## REFERENCES

- Acuna, J.: Improvements of U-Pipe Borehole Heat Exchangers, Diss, KTH, 2010.
- Amaya, A., Scherer, J., et al.: GreenFire Energy Closed-Loop Geothermal Demonstration using Supercritical Carbon Dioxide as Working Fluid. In Proceedings of the 45th Workshop on Geothermal Reservoir Engineering, Stanford, CA, USA, (2020).
- Landelle, A., Tauveron, N., ET AL.: Experimental Investigation of a Transcritical Organic Rankine Cycle with Scroll Expander for Low-Temperature Waste Heat Recovery, *Energy Procedia*, IV International Seminar on ORC Power Systems, Milano, Italy (2017).
- Holmberg, H., Acuna, J., et al.: Thermal evaluation of coaxial deep borehole heat exchangers, *Renewable Energy*, 97, (2016), 65-76.
- Khosravi, A., Syri, S., Zhao, X., Assad, M.E.H.: An artificial intelligence approach for thermodynamic modeling of geothermal based-organic Rankine cycle equipped with solar system, *Geothermics*, 80, (2019), 138–154.
- Karellas, S., Schuster, A.: Supercritical Fluid Parameters in Organic Rankine Cycle Applications. *Int. J. Thermodyn*, 11, (2008), 101–108.
- Olasolo, P., Juárez, M.C., et al.: Enhanced geothermal systems (EGS): A review, *Renewable and Sustainable Energy Reviews*, 56, (2016), 133-144.
- Pan, L., Wei, X., and Shi, W.: Performance analysis of a zeotropic mixture (R290/CO<sub>2</sub>) for trans-critical power cycle, *Chinese Journal of Chemical Engineering*, 23, (2015), 572-577.
- Sircar, A., Solanki, K., Bist, N., and Yadav, K.: Enhanced Geothermal Systems – Promises and Challenges, *Int. Journal of Renewable Energy Development (IJRED)*, 11(2), (2022), 333-346.
- Wu, C., Wang, S., Jiang, X., Li, J.: Thermodynamic analysis and performance optimization of transcritical power cycles using CO<sub>2</sub>-based binary zeotropic mixtures as working fluids for geothermal power plants, *Applied Thermal Engineering*, 115, (2017), 292-304.
- Zheng, S., Li, S., and Zhang, D.: Fluid and heat flow in enhanced geothermal systems considering fracture geometrical and topological complexities: An extended embedded discrete fracture model, *Renewable Energy*, 179, (2021), 163-178.
- Zhang, Y., Yu, C., Li, G., et al.: Performance analysis of a downhole coaxial heat exchanger geothermal system with various working fluids, *Applied Thermal Engineering*, 163, (2019), 114317.